PHYSICAL REVIEW B **86**, 201404(R) (2012)

# Stacking order, interaction, and weak surface magnetism in layered graphene sheets

Dong-Hui Xu,[1,*] Jie Yuan,[2,*] Zi-Jian Yao,[2] Yi Zhou,[1] Jin-Hua Gao,[3,2,†] and Fu-Chun Zhang[2,1]

[1]*Department of Physics, Zhejiang University, Hangzhou, 310027, China*

[2]*Department of Physics and Center of Theoretical and Computational Physics, The University of Hong Kong, Hong Kong, China*

[3]*Department of Physics, Huazhong University of Science and Technology, Wuhan, 430074, China*

(Received 30 July 2012; revised manuscript received 24 October 2012; published 7 November 2012)

Recent transport experiments have demonstrated that rhombohedral-stacking trilayer graphene is an insulator with an intrinsic gap of 6 meV and Bernal-stacking trilayer graphene is a metal. We propose a Hubbard model with a moderate $U$ for layered graphene sheets, and show that the model well explains the experiments on the stacking-dependent energy gap. The moderate on-site Coulomb repulsion drives the metallic phase of the noninteracting system to a weak surface antiferromagnetic insulator for the rhombohedral stacking layers, while the interaction-opened energy gaps for the Bernal stacking layers are much smaller.

DOI: 10.1103/PhysRevB.86.201404 PACS number(s): 73.22.Pr, 71.30.+h, 73.21.Ac, 75.70.Cn

In the past several years, the rapid development in preparing few-layer graphene samples has promoted great theoretical[1–13] and experimental[14–22] interest in such novel quasi-two-dimensional electron systems. Few-layer graphene may be a platform for many new physics issues and is of potential application in electronics. One peculiar feature of the layered graphene system is the stacking order, which offers a new route to manipulate the electronic properties in graphene layers.

The Bernal (or *ABA*) stacking and the rhombohedral (or *ABC*) stacking are two stable stacking orders observed in experiments. As shown in Fig. 1, in either *ABA* or *ABC* stacking order, the second graphene sheet is shifted by one bond length along the C-C bond direction. The third graphene sheet is shifted back and aligned with the first sheet in the *ABA* stacking, while it is shifted further by one more bond length along the same direction in the rhombohedral stacking. So the *ABA* stacking order is *ABABAB*..., and the rhombohedral stacking is *ABCABC*.... A trilayer graphene system is the minimal structure relevant for the stacking order.

The electronic structures of the graphene layers strongly depend on their stacking order.[1–4] In the *ABA*-stacking $N$-layer system, there are $N/2$ electronlike and $N/2$ holelike parabolic sub-bands touching at $\epsilon = 0$ for even $N$, and an additional sub-band with linear dispersion for odd $N$. The states in all the sub-bands are bulk states extending to all the layers. In the *ABC*-stacking layers, the low-energy electronic structure is described by two sub-bands with dispersion $\epsilon \sim k^N$ near the points $K$ and $K'$ in the two-dimensional (2D) Brillouin zone. These low-energy states are localized on the outermost layers, and are zero modes on the surfaces protected by the topology.[23,24] In two dimensions, the dispersion of $\epsilon(k) \sim k^N$ gives a density of states $D(\epsilon) \sim \epsilon^{-1+2/N}$, which is divergent for $N \geqslant 3$ at $\epsilon = 0$. This indicates a strong instability toward symmetry-broken states.[5,24]

Trilayer graphene systems are of particular interest for they represent the simplest case for investigating stacking-dependent graphene. Very recently, a stacking-dependent intrinsic gap in trilayer graphene has been observed in transport measurements.[21,22] In the charge-neutral case, namely, undoped trilayer samples, the experiments indicate that the *ABA*-stacking trilayer graphene is metallic, whereas the *ABC*-stacking trilayer graphene is insulating with an intrinsic gap of about 6 meV. Since the noninteracting electronic structures of both stacking orders are gapless and hence metallic, the experimental observation of the gap in the *ABC*-stacking trilayer is in sharp contrast with the noninteraction picture and points to the importance of the interaction in these systems.

In this Rapid Communication, we propose that the observed stacking-dependent metallic or insulting states can be explained by a Hubbard model with a moderate on-site Coulomb repulsion $U$. We use a self-consistent mean-field theory to show that the ground state of the *ABC*-stacking trilayer is a weak antiferromagnet with opposite ferrimagnetic orderings on the top and bottom layers, due to the divergent density of states in the metallic phase. The magnetic ordering opens a gap $\epsilon_g^{ABC}$, which compares well with the experimental data. For an *ABA*-stacking trilayer, the moderate on-site Coulomb interaction will also open a spin-density-wave (SDW) energy gap, but it is much smaller than that in *ABC*-stacking case and is hard to detect in transport measurements. Our theory is extended to study stacking-dependent graphene systems with larger numbers of layers. We have found that it is a general property that, in *ABC*-stacking layers, moderate on-site Coulomb interaction opens a sizable energy gap at the Fermi level (the maximum is about 20 meV depending on the number of the layer) and leads to a weak surface antiferromagnetic state, while the energy gap of the *ABA*-stacking layers is always smaller than 0.22 meV. These results can be further tested in future experiments.

We model $N$-layer graphene systems by using a Hubbard model $H = H_0 + H_U$, where $H_0 = H_{\text{intra}} + H_{\text{inter}}$ is a tight-binding Hamiltonian to describe the kinetic term of the system and $H_U$ describes the on-site Coulomb repulsion. The chemical potential is set to zero, and the average number of electrons per site is 1. The intralayer hopping term $H_{\text{intra}}$ is the tight-binding Hamiltonian of independent graphene sheets. For simplicity, we include only nearest-neighbor hoppings,[25]

$$H_{\text{intra}} = -t \sum_{l\langle ij\rangle\sigma} \{a_{l\sigma}^{\dagger}(i) b_{l\sigma}(j) + \text{H.c}\}, \tag{1}$$

where $a_{l\sigma}(i)$ and $b_{l\sigma}(j)$ are the annihilation operators of an electron on sublattices $A$ and $B$, respectively. $l$ denotes the layer index running from 1 to $N$, $\langle ij\rangle$ are nearest-neighbor

 

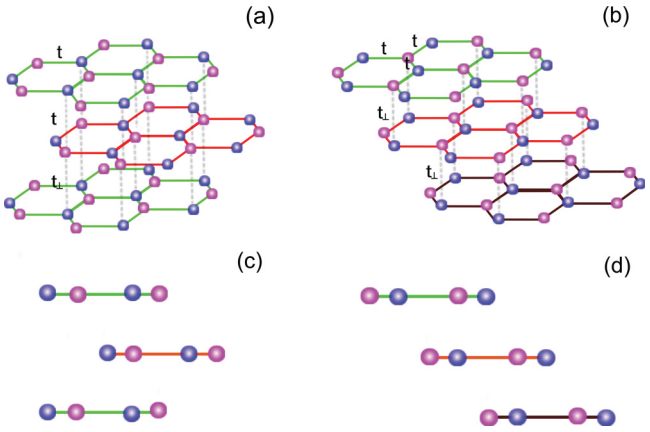


FIG. 1. (Color online) Schematic diagrams of trilayer graphene sheets. (a) Bernal (*ABA*) stacking and (b) rhombohedral (*ABC*) stacking. (c) and (d) are their side views. Blue and pink colors represent carbon atoms on sublattices $A$ and $B$, respectively.

pairs, and $\sigma$ is the spin. $H_{\rm inter}$ describes the interlayer hopping given by

$$H_{\rm inter}^{\rm R,B} = t_\perp \sum_{\langle ll'\rangle,\langle ii'\rangle\sigma} \{a_{l\sigma}^\dagger(i) b_{l'\sigma}(i') + {\rm H.c.}\} \qquad (2)$$

for the rhombohedral or Bernal stacking order. Here, $\langle ll'\rangle$ represents summation over the two adjacent layers, and $\langle ii'\rangle$ that over two sites aligned in adjacent layers as shown in Fig. 1. The Hubbard term $H_U = U\sum_{li} n_{l\uparrow}(i) n_{l\downarrow}(i)$ will be approximated by a mean-field Hamiltonian,

$$H_U^{\rm MF} = U \sum_{l,i\sigma} \langle n_{l\sigma}(i)\rangle n_{l\bar\sigma}(i), \qquad (3)$$

where $\bar\sigma = -\sigma$. $\langle n_{l\sigma}(i)\rangle$ is determined self-consistently. We consider a spin-density-wave state and introduce two mean fields on each layer $l$, one for sublattice $A$ and one for sublattice $B$, $\langle n_{l\uparrow}^{A,B}\rangle$. The mean fields for spin down are related to the spin-up ones, $\langle n_{l\downarrow}^{A,B}\rangle = 1 - \langle n_{l\uparrow}^{A,B}\rangle$. Note that we have examined possible charge-density-wave states within the model and found no evidence for their existence.

We first examine the trilayer graphenes ($N = 3$). The energy bands for the noninteracting models are shown in Fig. 2(a) for *ABC* stacking (solid red line) and in Fig. 2(b) for *ABA* stacking with parameters $t = 3.16$ eV and $t_\perp = 0.39$ eV. The noninteracting dispersion in Fig. 2(a) is $\epsilon \sim k^3$ at small $k$ for both conduction and valence bands, which gives rise to a divergent density of states $D(\epsilon) = \epsilon^{-1/3}$ at $\epsilon = 0$, and the wave functions for $k$ near the $K$ and $K'$ points are localized on the outer surfaces. The energy bands in Fig. 2(b) consist of a parabolic and a linear dispersion, neither of which is localized on the outer surfaces, and the density of states is a constant at $\epsilon = 0$. The energy gaps associated with SDW orderings are plotted in Fig. 2(c) as functions of $U$ for both the *ABC*- and *ABA*-stacking orders. In the presence of the Hubbard $U$, a SDW energy gap is opened for both *ABA*- and *ABC*-stacking trilayers. An interesting phenomenon is that, with the same $U$, the energy gap of the *ABC*-stacking trilayer is always much larger than that of the *ABA* trilayer [see Figs. 2(c) and 2(d)]. This distinction is attributed to their different densities of states near the Fermi level. The divergent density of states of the surface zero modes for the *ABC*-stacking graphene, protected by the momentum topology, actually induces its sensitivity to the interaction.

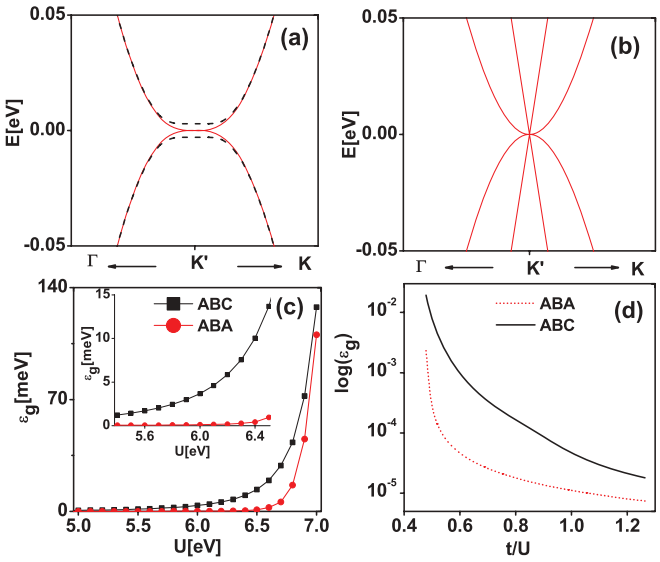


FIG. 2. (Color online) (a) Low-energy bands of *ABC*-stacking trilayer. Solid red line, $U = 0$; dashed black line, $U = 6.2$ eV. (b) Low-energy bands of *ABA* trilayer for $U = 0$. (c) Mean-field energy gaps as functions of $U$ for *ABC* and *ABA* trilayer graphene. (d) Logarithmic plots of energy gaps as functions of $t/U$. The parameters are $t = 3.16$ eV and $t_\perp = 0.39$ eV.

More quantitatively, there are three distinguished regions in $U$ for the gaps. At $U < 5.5$ eV, the gaps for both *ABA* and *ABC* stacking are tiny while the gap for *ABC* stacking is at least one order of magnitude larger than that for *ABA* stacking. At $5.5 < U < 6.4$ eV, the gap size grows rapidly to be observable (several meV) for the *ABC* stacking, but remains tiny for the *ABA* stacking (smaller than 0.2 meV). In this region, the *ABC*-stacking trilayer is insulating with an observable gap while the *ABA*-stacking trilayer remains conducting, considering that the temperature in transport measurements is about 1.5 K.[21] At $U > 6.4$ eV, the gaps for both *ABC*- and *ABA*-stacking orders become observable, and the srtructures become insulating. Actually the gaps for the two stacking orders become similar at $U > 7$ eV as we can see from Fig. 2(c). Experimentally, the transport data show that the *ABC*-stacking trilayer graphene is an insulator with a gap of 6 meV and the *ABA*-stacking trilayer is metallic. In comparison with the experiments, the mean-field calculations of the Hubbard model suggest that the Hubbard $U$ is within the interval of moderate values $5.5 < U < 6.4$ eV, i.e., $1.74t < U < 2.03t$.

In Fig. 2(a), we show the calculated quasiparticle dispersion for the *ABC*-stacking trilayer graphene for a choice of $U = 6.2$ eV (dashed black line). The corresponding gap is estimated to be $\epsilon_g \approx 5.8$ meV. Note that, with $U = 6.2$ eV, the corresponding energy gap of *ABA* stacking is about 0.18 meV. Our model and the calculations well explain the recent experiments showing a stacking-dependent energy gap in trilayer graphene. The experimentally observed energy gap may be used to estimate the value of $U$. Our mean-field theory suggests that $U \approx 6.2$ eV. More accurate numerical simulation may improve this estimate.

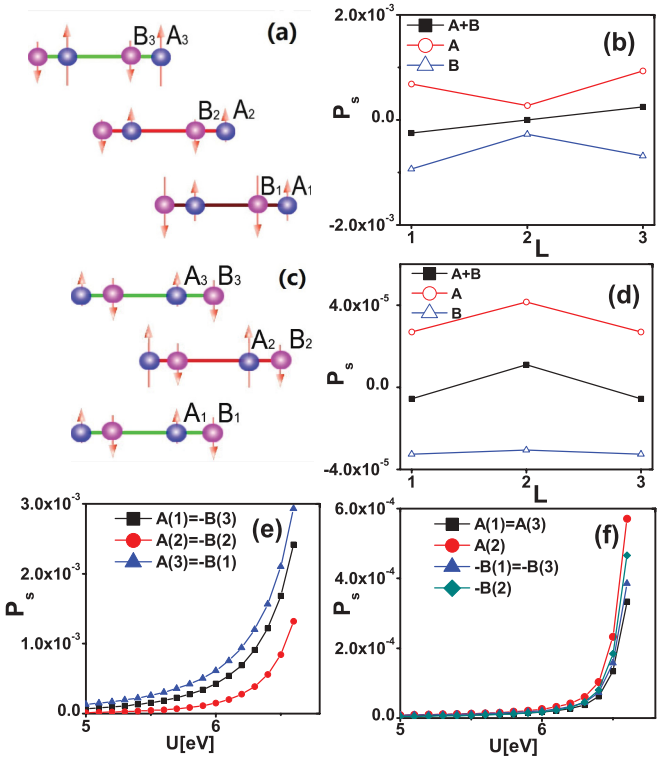


FIG. 3. (Color online) Schematic illustration of the spin ordering and spin polarization per site with $U = 6.2$ eV: (a) and (b) for *ABC*-stacking trilayer graphene, (c) and (d) for the *ABA*-stacking case. The spin polarization as a function of $U$: (e) for *ABC* stacking and (f) for *ABA* stacking.

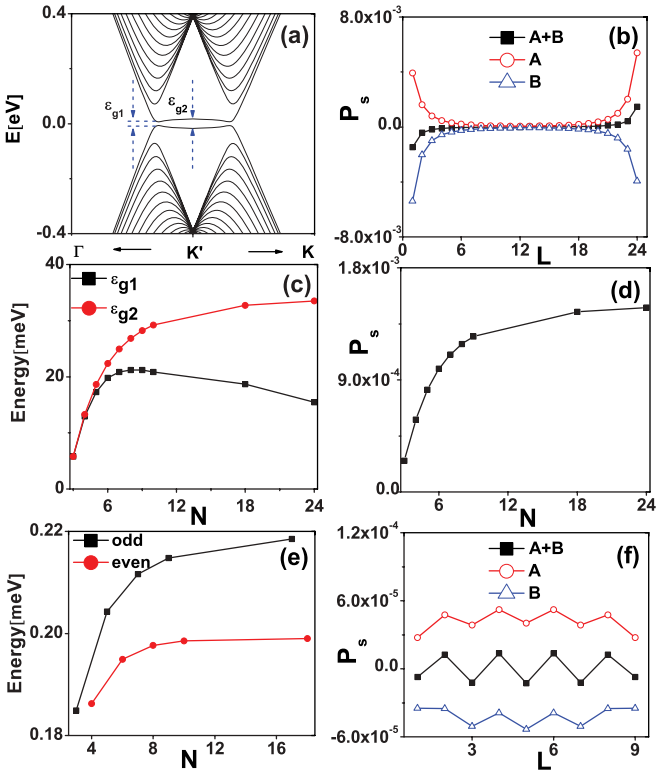


FIG. 4. (Color online) *ABC*-stacking $N$-layer graphene: (a) energy band and (b) spin polarization for $N = 24$; (c) the gaps $\epsilon_{g1}$ and $\epsilon_{g2}$; and (d) surface spin polarization as functions of $N$. *ABA*-stacking $N$-layer graphene: (e) energy gap as a function of $N$, and (f) spin polarization for $N = 9$. $U = 6.2$ eV and the hopping parameters are the same as in Fig. 2.

We now discuss the spin-density state and the spin polarization of the *ABC*-stacking layer. From the self-consistent mean-field theory we obtain the site spin polarization on sublattice $A$ or $B$, defined as $P_s(l,i) = \langle n_{l\uparrow}^{A,B} \rangle - \langle n_{l\downarrow}^{A,B} \rangle$. The calculated spin polarizations are plotted in Fig. 3(b), and the spin structure in the trilayer graphene is schematically illustrated in Fig. 3(a). The spin ordering is antiferromagnetic, where the neighboring spins (intra- or interlayer) are antiparallel to each other. However, there is a net spin polarization on the top or bottom layer, so each surface shows ferrimagnetic ordering. The spin polarization is mainly distributed on the two outer surfaces. In each layer, the spin polarizations on sublattices $A$ and $B$ have opposite directions. The net spin polarization is zero in the middle layer, and has opposite signs in the top and bottom layers. There is a symmetry of combined inversion and time reversal: $P_s(l = 1, i \in A(B)) = P_s(l = 3, i \in B(A))$. Note that the average spin polarization of the whole system is zero. For the parameters given in Fig. 3(b), the site spin polarizations in the top layer are about $6.9 \times 10^{-4}$ and $-9.6 \times 10^{-4}$ on sublattices $A$ and $B$, respectively, and the net spin polarization is $-2.5 \times 10^{-4}$ per site on average, which gives a surface magnetization of $0.005 \mu_B/\text{nm}^2$. The weak surface magnetization on the *ABC*-trilayer graphene is analogous to the ferromagnetic edge states in graphene zigzag ribbons,[26] in which the density of states of the flat band-edge states is divergent, inducing edge spin polarization in the presence of a weak interaction. The interaction-induced gap in graphene zigzag ribbons has been confirmed in a recent scanning tunneling microscope (STM) experiment.[27] We also show the spin polarization of the *ABC*-stacking trilayer as a function of $U$ in Fig. 3(e).

As a comparison, we discuss the corresponding spin-density state for *ABA* trilayer graphene. The results are shown in Figs. 3(c) and 3(d). The spin polarization of the *ABA*-stacking trilayer is rather tiny, nearly two orders of magnitude smaller than that of the *ABC*-stacking trilayer. The spin structure in the *ABA*-stacking case is also quite different, although the spin ordering is still antiferromagnetic. For each layer, there is a nonzero net spin polarization and the largest value appears in the middle layer. We see that the top and bottom layers are equivalent here, because of the mirror symmetry with respect to the middle layer. Note that the net spin polarization of the whole system is still zero. In Fig. 3(f), we give the spin polarization of the *ABA*-stacking trilayer as a function of $U$.

We now discuss $N > 3$ graphene layers. For *ABC*-stacking graphene layers and in the charge-neutral case, there is always an interaction-$U$-induced gap at the Fermi level with spontaneous surface spin-density-wave ordering. In Figs. 4(a) and 4(b), we show the results for $N = 24$ layers as an example. Since the minimum band gap ($\epsilon_{g1}$) is no longer at the $K$ or $K'$ point, as we can see from Fig. 4(a), we introduce a second gap $\epsilon_{g2}$ for the energy gap at the $K$ or $K'$ point. As shown in Fig. 4(b), the spin polarization is localized near the surfaces. In Fig. 4(c), we present the energy gaps as functions

of $N$. As $N$ increases, $\epsilon_{g1}$ first increases to approach its maximum of about 20 meV at $N = 9$, and then decreases to a value of 15 meV at $N = 24$. On the other hand, $\epsilon_{g2}$ increases with the layer thickness $N$ and reaches a saturated value of about 33 meV. The $N$-dependent spin polarization is shown in Fig. 4(d); it increases with the layer thickness, and approaches a saturated value, which is at least 5–6 times the surface magnetization in the trilayer case. Note that first-principles calculations involving a local-spin-density approximation have been applied to study eight-layer *ABC*-stacking graphene,[13] and found a spin-density-wave ground state. This result is consistent with the results of the Hubbard model proposed here, while our results are more general and distinguish different stacking orders.

We have also applied mean-field theory to study $N$-layer graphene with *ABA* stacking. The results are shown in Figs. 4(e) and 4(f). We see that the energy gaps of the *ABA*-stacking $N$-layer graphene samples are much smaller than those in the *ABC*-stacking cases, and the maximum value is smaller than 0.22 meV. Note that, for $N$-layer graphene with *ABA* stacking, there are two kinds of band structure depending on whether $N$ is even or odd. So we can observe an even-odd dependence of the energy gap in Fig. 4(e). However, the energy difference is smaller than 0.02 meV, which is quite hard to detect in experiment. We also calculate the corresponding spin polarizations. The spin ordering is still antiferromagnetic. Each layer has a net spin polarization, and the spin polarizations of the neighboring layers have opposite signs. In Fig. 4(f), we show the spin polarization of the $N = 9$ sample as an example. We should emphasize that, due to the small values of the energy gap and spin polarization, the most likely case is that *ABA*-stacking $N$-layer graphene is always metallic in experiment, which is in sharp contrast with the case of *ABC*-stacking $N$-layer graphene.

We argue that mean-field theory should give qualitatively or semiquantitatively correct physics for the stacking-dependent instability, or the insulating or metallic states in layered graphene, while more accurate calculations may refine the estimate of the value of $U$. We remark that the proposed Hubbard model with a moderate $U$ should capture the most important physics for the stacking-dependent ground states in layered graphene. We think that remote hopping cannot influence our picture of the experiments, since the on-site interaction $U$ is much larger than the remote hopping terms in the moderate-$U$ region. The picture in the small-$U$ region, where the interaction $U$ is comparable with the remote hopping terms, may be affected.[9] It is an interesting issue but unrealistic, and out of the scope of this paper. The intersite Coulomb repulsion has a tendency to drive the metallic phase to a charge-density-wave state, which is not compatible with the on-site $U$ studied in the present work. Since the intersite repulsion is weaker than the on-site Coulomb repulsion $U$, we may argue that that term may not be relevant. More exotic states such as quantum spin Hall and anomalous Hall states have been proposed in models with spin-orbit coupling or intersite interaction on a honeycomb lattice.[28,29] The possible realization of these exotic phases in layered graphene is highly interesting. In view of the very weak spin-orbit coupling in graphene,[30] more detailed study will be needed to explore the possibility. Note that, although unrelated to the stacking order, there have been various proposals for the interaction-driven correlated ground state of bilayer graphene.[31]

In summary, we have proposed a Hubbard model with a moderate $U$ to describe $N$-layer graphene, and applied mean-field theory to study the ground state and the excited energy gap of charge-neutral systems. The metallic state of the *ABC*-stacking layer is found to be unstable against any repulsion $U$ due to the divergent density of states at zero energy. Its ground state is a surface antiferromagnetic state with opposite ferrimagnetism on the top and bottom surfaces, which opens a gap. The energy gap is estimated to be 5.8 meV for $U = 6.2$ eV for $N = 3$. The metallic ground state of the *ABA*-stacking layer is also unstable against the on-site Coulomb repulsion, while the energy gap is at least one order of magnitude smaller than that for *ABC* stacking, which is too small to detect even at moderate $U$. Our model and calculations well explain recent transport experiments, showing that *ABC*-stacking trilayer graphene is an insulator with a gap about 6 meV, and *ABA*-stacking trilayer graphene remains metallic. The spin polarization in the spin-ordered state is found to be weak, but should be measurable. We also apply our model to study layered graphene systems with large layer number ($N > 3$). We find that the *ABC*-stacking graphene multilayer has a sizable interaction-induced energy gap at the Fermi level while the interaction-opened energy gap for the *ABA*-stacking multilayer is always tiny. This prediction can be tested in future experiments.

*Note added.* Recently, we learned about the work of Jung and MacDonald,[32] Liu *et al.*,[33] Scherer *et al.*,[34] and Cvetkovic and Vafek,[35] in which the ground states of graphene trilayers have been discussed from different points of view.

We acknowledge some financial support from HKSAR RGC Grant No. HKU 701010 and CRF Grant No. HKU 707010. J.H.G. is supported by the National Natural Science Foundation of China (Project No. 11274129). D.H.X. and Y.Z. are supported by the National Basic Research Program of China (973 Program, Grant No. 2011CBA00103), the NSFC (Grant No. 11074218), and the Fundamental Research Funds for the Central Universities in China.

*D.-H.X. and J.Y. contributed equally to this work.

†jhgao1980@gmail.com

[1] F. Guinea, A. H. Castro Neto, and N. M. R. Peres, Phys. Rev. B **73**, 245426 (2006); A. H. C. Neto, F. Guinea, N. M. R. Peres, K. S. Novoselov, and A. K. Geim, Rev. Mod. Phys. **81**, 109 (2009).

[2] S. Latil and L. Henrard, Phys. Rev. Lett. **97**, 036803 (2006).

[3] B. Partoens and F. M. Peeters, Phys. Rev. B **74**, 075404 (2006); **75**, 193402 (2007).

[4] H. Min and A. H. MacDonald, Phys. Rev. B **77**, 155416 (2008); F. Zhang, B. Sahu, H. Min, and A. H. MacDonald, *ibid.* **82**, 035409 (2010).

[5] F. Zhang, J. Jung, G. A. Fiete, Q. Niu, and A. H. MacDonald, Phys. Rev. Lett. **106**, 156801 (2011); F. Zhang, D. Tilahun, and A. H. MacDonald, Phys. Rev. B **85**, 165139 (2012).

[6] A. A. Avetisyan, B. Partoens, and F. M. Peeters, Phys. Rev. B **80**, 195401 (2009).

[7]M. Koshino and E. McCann, Phys. Rev. B **80**, 165409 (2009); M. Koshino, *ibid.* **81**, 125304 (2010).
[8]S. B. Kumar and J. Guo, Appl. Phys. Lett. **98**, 222101 (2011).
[9]M. Koshino and E. McCann, Phys. Rev. B **83**, 165443 (2011).
[10]J.-A. Yan, W. Y. Ruan, and M. Y. Chou, Phys. Rev. B **83**, 245418 (2011).
[11]S. B. Kumar and J. Guo, Appl. Phys. Lett. **100**, 163102 (2012).
[12]T. Wakutsu, M. Nakamura1, and B. Dóra, Phys. Rev. B **85**, 033403 (2012).
[13]M. Otani, M. Koshino, Y. Takagi, and S. Okada, Phys. Rev. B **81**, 161403 (2010); M. Otani, Y. Takagi, M. Koshino, and S. Okada, Appl. Phys. Lett. **96**, 242504 (2010).
[14]M. F. Craciun, S. Russo, M. Yamamoto, J. B. Oostinga, A. F. Morpurgo, and S. Tarucha, Nat. Nanotechnol. **4**, 383 (2009).
[15]T. Taychatanapat, K. Watanabe, T. Taniguchi, and P. Jarillo-Herrero, Nat. Phys. **7**, 621 (2011).
[16]A. Kumar, W. Escoffier, J. M. Poumirol, C. Faugeras, D. P. Arovas, M. M. Fogler, F. Guinea, S. Roche, M. Goiran, and B. Raquet, Phys. Rev. Lett. **107**, 126806 (2011).
[17]L. Zhang, Y. Zhang, J. Camacho, M. Khodas, and I. Zaliznyak, Nat. Phys. **7**, 953 (2011).
[18]K. F. Mak, J. Shan, and T. F. Heinz, Phys. Rev. Lett. **104**, 176404 (2010).
[19]C. H. Lui, Z. Q. Li, K. F. Mak, E. Cappelluti, and T. F. Heinz, Nat. Phys. **7**, 944 (2011).
[20]Z. Li, C. H. Lui, E. Cappelluti, L. Benfatto, K. F. Mak, G. L. Carr, J. Shan, and T. F. Heinz, Phys. Rev. Lett. **108**, 156801 (2012).
[21]W. Bao, L. Jing, J. Velasco, Jr., Y. Lee, G. Liu, D. Tran, B. Standley, M. Aykol, S. B. Cronin, D. Smirnov, M. Koshino, E. McCann, M. Bockrath, and C. N. Lau, Nat. Phys. **7**, 948 (2011).
[22]S. H. Jhang *et al.*, Phys. Rev. B **84**, 161408(R) (2011).
[23]T. T. Heikkil, N. B. Kopnin, and G. E. Volovik, JETP Lett. **94**, 233 (2011).
[24]N. B. Kopnin, T. T. Heikkila, and G. E. Volovik, Phys. Rev. B **83**, 220503(R) (2011); N. B. Kopnin, JETP Lett. **94**, 81 (2011).
[25]The small values of the longer-range hopping integrals do not change the basic conclusion presented here.
[26]Y.-W. Son, M. L. Cohen, and S. G. Louie, Phys. Rev. Lett. **97**, 216803 (2006).
[27]C. G. Tao, L. Y. Jiao, O. V. Yazyev, Y.-C. Chen, J. J. Feng, X. W. Zhang, R. B. Capaz, J. M. Tour, A. Zettl, S. G. Louie, H. J. Dai, and M. F. Crommie, Nat. Phys. **7**, 616 (2011).
[28]S. Raghu, X.-L. Qi, C. Honerkamp, and S.-C. Zhang, Phys. Rev. Lett. **100**, 156401 (2008).
[29]C. L. Kane and E. J. Mele, Phys. Rev. Lett. **95**, 146802 (2005).
[30]Y. Yao, F. Ye, X. L. Qi, S. C. Zhang, and Z. Fang, Phys. Rev. B **75**, 041401(R) (2007).
[31]J. Nilsson, A. H. Castro Neto, N. M. R. Peres and F. Guinea, Phys. Rev. B **73**, 214418 (2006); H. Min, G. Borghi, M. Polini, and A. H. MacDonald, *ibid.* **77**, 041407 (2008); Y. Lemonik, I. L. Aleiner, C. Toke, and V. I. Falko, *ibid.* **82**, 201408 (2010); O. Vafek and K. Yang, *ibid.* **81**, 041401 (2010); R. Nandkishore and L. Levitov, Phys. Rev. Lett. **104**, 156803 (2010); F. Zhang, H. Min, M. Polini, and A. H. MacDonald, Phys. Rev. B **81**, 041402 (2010); J. Jung, F. Zhang, and A. H. MacDonald, *ibid.* **83**, 115408 (2011); O. Vafek, *ibid.* **82**, 205106 (2010); M. Kharitonov, arXiv:1109.1553; M. M. Scherer, S. Uebelacker, and C. Honerkamp, Phys. Rev. B **85**, 235408 (2012); E. V. Gorbar, V. P. Gusynin, V. A. Miransky, and I. A. Shovkovy, *ibid.* **86**, 125439 (2012); F. Zhang, H. Min, and A. H. MacDonald, *ibid.* **86**, 155128 (2012); T. C. Lang, Z. Y. Meng, M. M. Scherer, S. Uebelacker, F. F. Assaad, A. Muramatsu, C. Honerkamp, and S. Wessel, Phys. Rev. Lett. **109**, 126402 (2012).
[32]J. Jung and A. H. MacDonald, arXiv:1208.0116.
[33]Haiwen Liu, Hua Jiang, X. C. Xie, and Qing-feng Sun, Phys. Rev. B **86**, 085441 (2012).
[34]M. M. Scherer, S. Uebelacker, D. D. Scherer, and C. Honerkamp, Phys. Rev. B **86**, 155415 (2012).
[35]V. Cvetkovic and O. Vafek, arXiv:1210.4923.